

Unusual near-threshold potential behavior for the weakly bound nucleus ${}^9\text{Be}$ in elastic scattering from ${}^{209}\text{Bi}$

C. Signorini,¹ A. Andrighetto,¹ M. Ruan,² J. Y. Guo,¹ L. Stroe,¹ F. Soramel,³ K. E. G. Löbner,⁴ L. Müller,¹ D. Pierroutsakou,⁵ M. Romoli,⁵ K. Rudolph,⁴ I. J. Thompson,⁷ M. Trotta,⁵ A. Vitturi,¹ R. Gernhäuser,⁶ and A. Kastenmüller⁶

¹Physics Department of University and INFN, via Marzolo 8, I-35131 Padova, Italy

²INFN, Laboratori Nazionali di Legnaro, I-35020 Legnaro, Padova, Italy

³Physics Department of University and INFN, via delle Scienze 208, I-33100 Udine, Italy

⁴Sektion Physik, Ludwig-Maximilians-University München, D-85748 Garching, Germany

⁵Physics Department of University and INFN, via Cintia, Monte S. Angelo, I-80125 Napoli, Italy

⁶Physics Department, Technical University München, D-85748 Garching, Germany

⁷Physics Department, University of Surrey, Guildford GU2 5XH, United Kingdom

(Received 20 December 1999; published 18 May 2000)

The cross sections for elastic scattering of the weakly bound ${}^9\text{Be}$ on ${}^{209}\text{Bi}$ around the Coulomb barrier have been measured with $\sim 5\%$ absolute accuracy from 40 to 48 MeV. The potential obtained from an optical model analysis has an unusual behavior. At the strong absorption radius the imaginary (absorptive) potential is increasing (rather than decreasing) with decreasing energy, as would be consistent with a long range polarization potential arising mainly from couplings to breakup channels. The real part, on the other hand, displays a strong attractive polarization contribution with the maximum at the barrier, as would be normally expected from a polarization contribution arising from strong couplings. The inelastic multiplet in ${}^{209}\text{Bi}$ of collective nature around 2.6 MeV, originating from the coupling [${}^{208}\text{Pb}(3^-) \otimes h_{9/2^-}$] J^π , was seen only at 48 MeV. The total multiplet cross section is well reproduced by coupled channel calculations with the potential obtained from the optical analysis and the experimental $B(E3)$ strengths of the ${}^{209}\text{Bi}$ multiplet levels.

PACS number(s): 25.70.Bc, 24.10.Eq

Due to the increasing interest in physics with radioactive nuclear beams, the interaction of weakly bound or halo nuclei at colliding energies around the Coulomb barrier is a very lively topic. In fact, among radioactive nuclei there are most of the best candidates for such investigations, and they will be more numerous in the future. The most relevant question is whether there is any signature of the expected influence of the weak binding, plus the eventual halo structure, on the various processes going on at the barrier energies, namely scattering (elastic and inelastic), transfer, breakup, and fusion. All of these nonelastic processes influence, to some extent, the entrance channel optical potential, so measurement of elastic scattering is a necessary first step.

Within this research framework, systematic investigations are going on in the systems ${}^9\text{Be}+{}^{209}\text{Bi}$, ${}^{208}\text{Pb}$ for the following reasons: (i) ${}^{11}\text{Be}$ is a weakly bound unstable nucleus, $S_n=0.50$ MeV, with a well established halo structure [1], and a low energy radioactive beam has already been developed [2,3] for this isotope. (ii) ${}^{208}\text{Pb}$ and ${}^{209}\text{Bi}$ have very well established shell model structures, constitute two ‘‘easy’’ low cost targets from an experimental view point, and are easy to be treated theoretically. (iii) ${}^9\text{Be}$ represents a reference stable nucleus with which high precision measurements are possible due to the much higher beam intensity achievable. Moreover, the ${}^9\text{Be}$ nucleus is quite interesting by itself, since it is one of the two less bound stable nuclei with $S_n=1.67$ MeV, the other one being ${}^6\text{Li}$ with $S_\alpha=1.47$ MeV.

The fusion process was extensively studied in the systems ${}^9,{}^{10},{}^{11}\text{Be}+{}^{209}\text{Bi}$ [2,4,5] and ${}^9\text{Be}+{}^{208}\text{Pb}$ [6]. One important finding in all these experiments is that the breakup process of both ${}^9\text{Be}$ and ${}^{11}\text{Be}$ projectiles has a significant influence on

the fusion one. Our systematic work therefore continued with precision measurements of the elastic scattering cross section of the ${}^9\text{Be}+{}^{209}\text{Bi}$ system around the Coulomb barrier. The goal was to get the interaction potential from a consistent optical model analysis, and then to look for possible signatures of the breakup process.

Some theoretical work done for a similar system ${}^{11}\text{Be}+{}^{197}\text{Au}$ [7,8] predicts a hindrance, i.e., ‘‘stronger’’ absorption, of $d\sigma/d\sigma_R$ at the barrier, $E({}^{11}\text{Be})=40$ MeV, and no hindrance below, $E({}^{11}\text{Be})=30$ MeV. The optical model analysis of the ${}^6,{}^7\text{Li}+{}^{208}\text{Pb}$ elastic scattering [9] shows, for the ${}^6\text{Li}$ projectile, that the imaginary (absorptive) potential at the distance corresponding to the strong interaction radius increases with decreasing energy, but not for ${}^7\text{Li}$. This should reflect the fact that ${}^6\text{Li}$ with $S_\alpha=1.47$ MeV can break more easily than ${}^7\text{Li}$ with $S_\alpha=2.47$ MeV as discussed also in Ref. [10]. The behavior of ${}^9\text{Be}$ optical potential near the barrier is predicted [10] to be close to that of ${}^6\text{Li}$ since both nuclei have similar breakup thresholds. Indeed the analysis of elastic scattering of ${}^6\text{Li}$, ${}^9\text{Be}$, as well as ${}^7\text{Li}$ by light targets shows that the real potentials, calculated with the double folding procedure, have to be all renormalized by a factor of ~ 0.5 in order to reproduce the data [11–13].

The elastic scattering data were taken using the Tandem Van de Graaff accelerator of the Munich Universities. Angular distributions were measured at ${}^9\text{Be}$ bombarding energies of 40, 42, 44, 46, and 48 MeV. The ${}^9\text{Be}$ 4^+ beam currents were ranging from 2 nA to 25 nA (electrical) on target depending on bombarding energies and scattering angles. The incoming beam was well defined in direction by means of a 4.5 mm diameter collimator located at ~ 18 cm from the

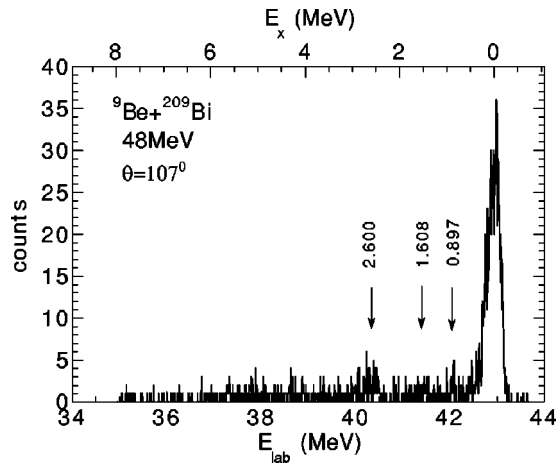


FIG. 1. Spectrum from ${}^9\text{Be}$ scattering by ${}^{209}\text{Bi}$ at 48 MeV recorded at 107° . The arrows indicate the location of the (expected) peaks from inelastic excitation of the first and second excited levels at 0.897 and 1.608 MeV and of the observed “ 3^- multiplet” at around 2.6 MeV of ${}^{209}\text{Bi}$. The ${}^9\text{Be}$ excitations cannot show up in this energy range since they correspond only to unbound states which decay into the $\alpha + \alpha + n$ channel.

target corresponding to an angular definition better than 0.7° . The targets used were $\sim 300 \mu\text{g}/\text{cm}^2$ natural Bismuth vacuum deposited onto $\sim 10 \mu\text{g}/\text{cm}^2$ carbon backing. An array of six identical silicon surface barrier detectors 300 μm thick was employed in the measurement. The detectors were all positioned 25 cm from the target, at a fixed angle of 7° from each other and spanning an angle of 1.4° defined by means of a 6 mm diameter collimator. The corresponding solid angle was 0.45 msr. A high precision machining of the mechanical support guaranteed that all solid angles were identical. With this arrangement it was possible to build up an overlapping set of elastic scattering angular distribution data at each bombarding energy in a reasonable time with an angular step of 3.5° . The most backward angle reached by the detectors was 156° , as imposed by the collimator geometry. Two monitor detectors, 300 μm thick, were located at $\pm 30^\circ$ and at a distance of 25 cm from the target covering a solid angle of 0.200 msr.

A typical spectrum collected at 48 MeV and 107° is shown in Fig. 1. The energy resolution of around 260 keV of all detectors, corresponding to $\Delta E/E \approx 0.6\%$, allowed an accurate determination of the elastic scattering peak. The arrows in Fig. 1 indicate the expected positions of the first two excited states, of single particle structure, ${}^{209}\text{Bi}$ at 0.897 MeV ($J^\pi = 7/2^-$) and 1.608 MeV ($J^\pi = 13/2^-$). In Fig. 1 a structure at $E_x \approx 2.6$ MeV assigned to the well established collective multiplet [${}^{208}\text{Pb}(3^-) \otimes h_{9/2}$] J^π with energies ranging from 2.492 to 2.741 MeV is clearly visible; the detectors resolution did not allow the separation of the seven levels. This assignment was also based on a similar observation in the scattering of ${}^{11}\text{B}$ by ${}^{209}\text{Bi}$ at $E \geq 51$ MeV [14]. The multiplet excitation could be observed clearly only at 48 MeV and barely at 46 MeV, where the statistics did not allow to extract any angular distribution data.

The overall data normalization for the absolute cross section determination was done at each energy assuming that

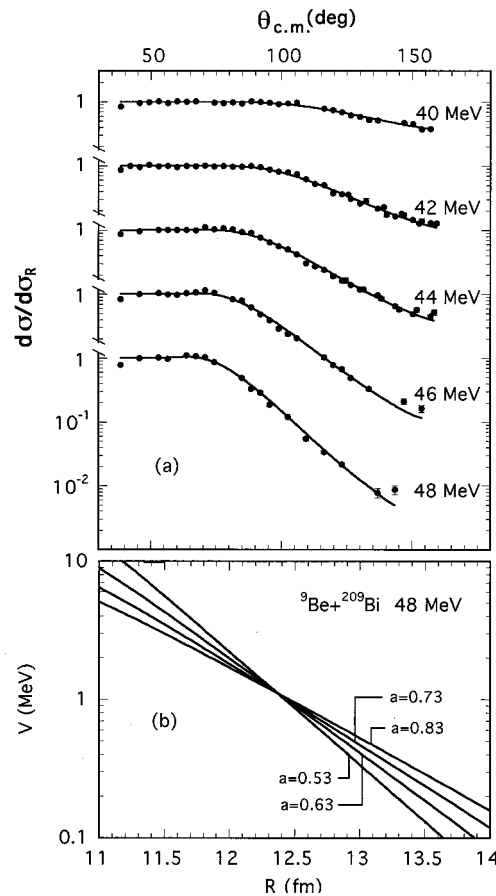


FIG. 2. (a) Angular distribution of ${}^9\text{Be}$ scattered elastically by ${}^{209}\text{Bi}$. The continuous lines are the result of the optical model fit with the code PTOLEMY with the parameters in Table I. Identical results are obtained with the code FRESKO and the parameters of Table I; (b) behavior of the real part of the potential fitting the 48 MeV elastic scattering data for different values of the diffuseness parameter.

the monitor detectors were measuring Rutherford scattering as confirmed by the experimental results; the solid angles were taken, in a first analysis step, from the detectors geometry and then slightly adjusted considering the angular region where $d\sigma/d\sigma_R = 1$. This leads to an estimated error in the absolute normalization of $\pm 5\%$. Figure 2(a) shows the obtained elastic scattering angular distributions; the overall absolute angle accuracy is estimated to be $\sim 1^\circ$. The error bars take into account only the statistical contribution and are smaller than the point dimension in most cases; they are visible only at the largest angles at 46 and 48 MeV. No rainbow peaks or Coulomb-nuclear interference dips are visible in Fig. 2(a). Figure 3 shows the 3^- multiplet angular distribution; at angles smaller than $\sim 90^\circ$ this multiplet could not be observed due to increasing background most probably originating from the tail of the elastic peak.

The experimental results were analyzed with the help of two different codes: PTOLEMY [15], for the elastic data since it has a parameter fitting built in routine, and FRESKO [16], mainly for the inelastic excitations, since it is a coupled channel code which can handle very large angular momentum ranges. The main goal of this analysis was to get con-

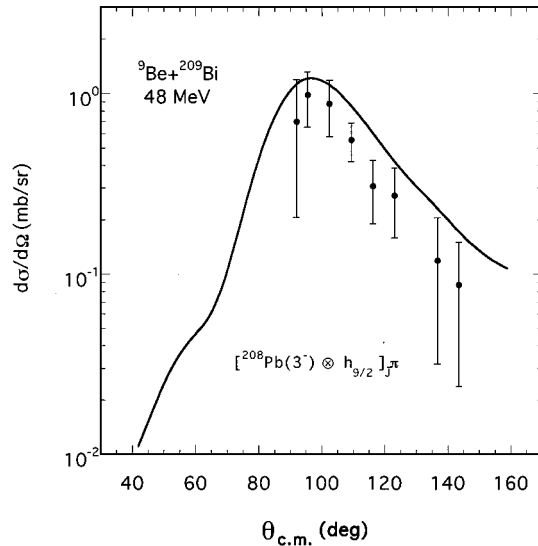


FIG. 3. Angular distribution of the inelastic collective multiplet at around 2.6 MeV originating from the coupling of the 3^- octupole excitation in ^{208}Pb with one proton in the $1h_{9/2}$ single particle state. The continuous line is the prediction of the FRESKO code calculated with the parameters of Table I and experimental $B(E3)$ values.

sistent optical potential parameter sets, and in particular to define the potential around the strong absorption radius. It is well known that at these energies the usual ambiguities common to all analyses of complex ion elastic scattering will be reflected by a nonunique set of parameters deduced from the fits, but the potential values at the strong absorption radius are usually well defined and rather independent upon these ambiguities, since the elastic scattering cross sections are sensitive mostly to this region, corresponding to a surface interaction of the two colliding nuclei.

A consistent optical model analysis was carried out for the elastic scattering data with the code PTOLEMY with a Woods-Saxon form real and imaginary potential. There are 6 parameters to be determined: V_0 (W_i), r_0 (r_i), a_0 (a_i), which are, respectively, the potential depth, the radius, and the diffuseness of the real (imaginary) potential. The total radius r is given by the usual formula $r = r_0(A_1^{1/3} + A_2^{1/3})$, where $A_1 = 9, A_2 = 209$. A two step fitting procedure was adopted. In the first step a grid search was done with four parameters fixed, $r_0 = r_i = 1.178$ fm, $a_0 = a_i = 0.63$ fm, and the remaining two V_0 and W_i as variables with starting point

52.2 MeV and $W_i = V_0$, respectively. The values of the parameters r_0, a_0, V_0 were obtained from the Akyüz-Winther potential [17]. In the second step r_0 and a_0 were kept fixed at the same value given above, and the other four parameters were varied with the output of the previous search used as a starting point. The parameters with their relative statistical errors obtained from the fitting procedure are listed in Table I. The fitting results are shown in Fig. 2(a) by continuous lines. In Table I are reported also the strong absorption radii calculated in two ways: (i) impact parameter corresponding to the scattering angle for which $d\sigma/d\sigma_R = 1/4$, (ii) radial distance at which the real potential is independent on realistic variations of the well parameters. An example of this is shown in Fig. 2(b) where the real potentials at 48 MeV resulting from the angular distribution fits with a_0 ranging from 0.53 to 0.83 fm are drawn. The results of these two procedures agree very well with each other. The real and imaginary potentials were then evaluated at an intermediate $r_{sa} = 12.5$ fm and plotted in Figs. 4(a),(c). Since the elastic scattering process is sensitive mainly to the surface potential, i.e., at r_{sa} , this is the only distance which has a clear physical meaning. In these two figures we show in addition the potentials for the very similar system $^9\text{Be} + ^{208}\text{Pb}$ at 50 MeV [18] and as a reference the values at the same distance of the bare Akyüz-Winther [17] potential (dashed line) and of the double folding potential with the $M3Y$ interaction (dashed-dotted line). For the folding potential the ^9Be density was included in the calculations with the same procedure adopted in Ref. [12]. For comparison the corresponding results obtained for $^6\text{Li} + ^{208}\text{Pb}$ [9] are also shown in Figs. 4(b),(d). Note that for both systems the double folding procedure based on realistic densities distributions for both ^9Be and ^6Li gives a potential value almost double with respect to the ‘‘global’’ behavior given by the Akyüz-Winther parametrization.

We observe that the real part of the ^9Be potential has a maximum around the barrier with a strong renormalization with respect to the bare potential. Such a large attractive polarization potential is consistent with the expectation [19] of ‘‘standard’’ polarization potential in the presence of strong coupling to excited states. The situation is less clear in the case of ^6Li , where the potential shows a maximum at the barrier energy, but with values smaller with respect to the predictions of the folding model, at variance therefore with the ^9Be case.

TABLE I. Woods-Saxon potential parameters obtained with a four-parameters fit, fixing $r_0 = 1.178$ fm and $a_0 = 0.63$ fm. Strong absorption radii deduced from $d\sigma/d\sigma_R = 1/4$ ($r_{\theta_{1/4}}$) and from a grid search on the fitting procedure (r_{sa}).

E_{lab} (MeV)	V_0 (MeV)	W_i (MeV)	r_i (fm)	a_i (fm)	$\chi^2/\text{deg.}$	χ^2/point	$r_{\theta_{1/4}}$ (fm)	r_{sa} (fm)
40.0	49.4 ± 3.8	132.0 ± 3.6	1.182 ± 0.002	0.621 ± 0.003	2.05	1.76	-	12.14
42.0	112.5 ± 1.0	168.7 ± 4.8	1.208 ± 0.002	0.541 ± 0.002	5.34	4.79	12.46	12.37
44.0	143.7 ± 1.2	186.3 ± 7.6	1.250 ± 0.002	0.439 ± 0.004	2.20	1.94	12.44	12.67
46.0	137.5 ± 1.4	139.2 ± 5.5	1.241 ± 0.002	0.458 ± 0.005	2.37	1.95	12.46	12.57
48.0	115.0 ± 1.5	98.9 ± 4.7	1.210 ± 0.003	0.545 ± 0.007	2.72	2.08	12.46	12.34

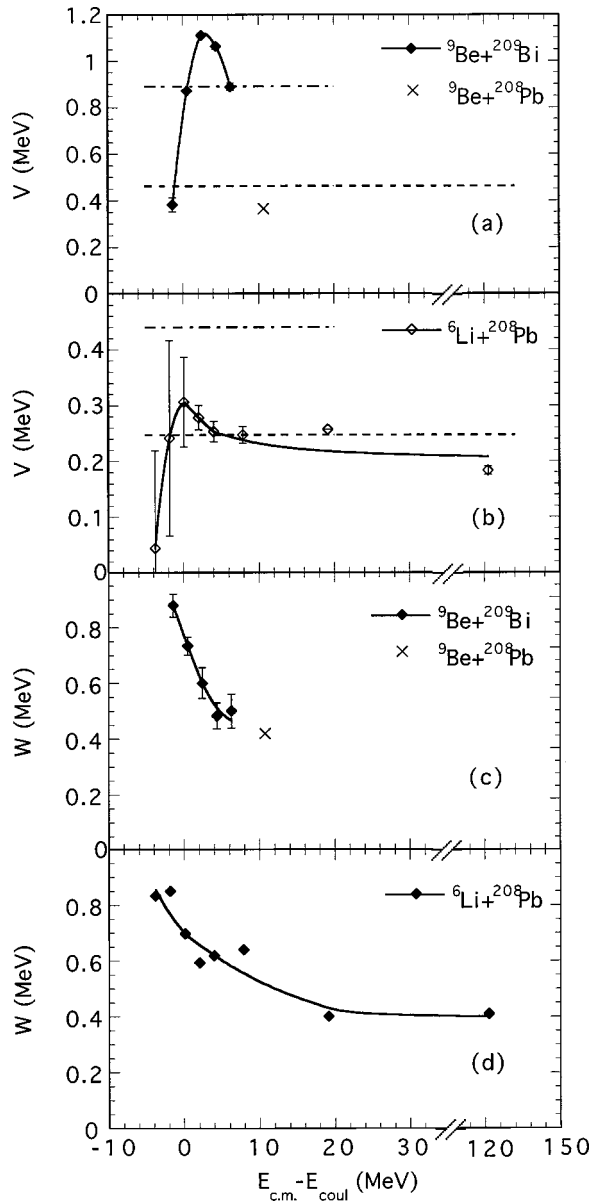


FIG. 4. Real (a),(b) and imaginary (c),(d) potentials calculated around the strong absorbing radii of the two systems. The ${}^6\text{Li}$ data are deduced from Fig. 2 of Ref. [9]. The dashed (dot-dashed) lines in (a),(b) show the value of the “bare” Akyüz-Winther potential (folding potential).

The imaginary/absorptive part increases with decreasing energies, even below the barrier where the fusion cross section decreases exponentially [5]; in this case the behavior, although different from the usual polarization case, is very similar to the ${}^6\text{Li}$ one. For ${}^9\text{Be}$ we cannot obviously draw any conclusion about threshold anomaly, absent with ${}^6\text{Li}$ projectile [13] as explained by intuitive theoretical arguments [20], because there are not enough experimental points. This analysis suggests anyhow that the polarization effect continues to dominate the coupling interaction down to and most likely below the Coulomb barrier. This behavior is quite different from that observed with well bound nuclei, where with decreasing energy the imaginary potential de-

creases since the inelastic excitations go to zero. This indicates that strong absorption channels are still open. Since the ${}^{209}\text{Bi}$ inelastic channels were found to have rather small cross sections this can be most likely related to the projectile breakup expected to be relevant for both ${}^9\text{Be}$ and ${}^6\text{Li}$ nuclei due to their low binding energies; if this is the case this breakup interaction should be predominantly of Coulomb type since we are at energies below barrier, even if nuclear breakup for weakly bound systems is expected to still be active at much larger distances than in normal cases. The contribution also of the reorientation coupling of the ${}^9\text{Be}$ ground state quadrupole, fairly large, cannot be excluded; such effect has been reported for the scattering of ${}^9\text{Be}$ by ${}^{40}\text{Ca}$ [11] and ${}^{44}\text{Ca}$, ${}^{39}\text{K}$ [12].

The above considerations are supported by the fact above the barrier that in the case of ${}^9\text{Be}$ the fusion cross section with ${}^{209}\text{Bi}$ appears to be hindered [5] as well as with ${}^{208}\text{Pb}$ [6], moreover in this last case also a sizable incomplete fusion cross section (due to breakup fragments) is reported. In the case of ${}^6\text{Li} + {}^{208}\text{Pb}$ a sizable breakup partial cross section (proceeding only via excitation of the first excited unbound 3^+ state at ~ 2.2 MeV, the so-called sequential breakup) was measured [21] to have a value raising from 3.0 mb at 23 MeV to 65 mb at 48 MeV. Finally, the analysis of the elastic scattering of polarized ${}^6\text{Li}$ and ${}^7\text{Li}$ by lighter targets needs the coupling to continuum (breakup) projectile states [22].

In order to have a more complete understanding of our data we have tried to describe the excitation of the unresolved “ 3^- ” ${}^{209}\text{Bi}$ multiplet (experimentally observed only at 48 MeV) with calculations which considered: (i) only DWBA first order coupling, (ii) “exact” coupled channel (CC) coupling. Both calculations included only the nine lowest ${}^{209}\text{Be}$ states, seven of which belong to the 3^- multiplet. Both calculations were done with the code FRESKO, the only one that can handle the extremely large angular momentum space necessary since ${}^9\text{Be}$ g.s. has $J^\pi = 3/2^-$, the ${}^{209}\text{Bi}$ states spins range from $3/2$ up to $15/2$ and a total spin, including the orbital angular momentum of the relative motion, up to $50\hbar$ had to be considered. The calculations were done with the potential given in Table I for 48 MeV and the coupling strengths deduced from the experimental $B(E3)$ values [23] known with precision between 10% and 20%, with no free parameters. In the case of CC approach, these are simplified calculations since they do not include explicitly the coupling to the ${}^9\text{Be}$ excited states, which are all unbound, leading to breakup, and to the ${}^9\text{Be}$ g.s. quadrupole moment which plays a relevant role as reported for the scattering by lighter isotopes [11,12]. We are well aware that there is a strong influence of ${}^9\text{Be}^*$ states on the scattering as evident from our fitted optical potential which has a large absorption term. This contribution is already built in an average way into the optical model potential adopted in the CC calculations for the “ 3^- ” ${}^{209}\text{Bi}$ multiplet.

The CC calculations results are shown in Fig. 3 by the continuous line obtained by adding the cross sections calculated for each single multiplet level. The DWBA results are equal within 5%. Within the accuracy of the experimental points and $B(E3)$ values these calculations reproduce the inelastic data, especially the maximum of the cross section in

value and angular position. The elastic cross section is also reproduced by the CC approach; the values coincide with the optical model fit reported in Fig. 2 for the 48 MeV data. The fact that the CC calculations reproduce the elastic and inelastic data, which have a small cross section ~ 5 mb, $< 0.5\%$ of the total reaction cross section, justifies, in our opinion, this general CC approach too. Therefore the effect of the considered coupling on the elastic channel is small and the “bare” potential required for these specific model calculations is quite similar to the fitted optical model one. Thus the experimental results are fairly well understood in the frame of the available well established approaches.

A direct measurement of the total breakup cross section in the ${}^9\text{Be} + {}^{209}\text{Bi}$ system would be very useful for a more quantitative understanding of the interaction process at the barrier and for a correct interpretation in the frame of a full coupled channel calculation approach.

In summary, the elastic scattering cross section of ${}^9\text{Be}$ by ${}^{209}\text{Bi}$ was measured with high accuracy from 40 to 48 MeV. The fitted optical potential shows, around the strong absorp-

tion radius, a strong attractive real polarization peaked at the barrier and an imaginary/absorbing part increasing with decreasing energy, consistent with a coupling to excited ${}^9\text{Be}$ states which is extending its action below the Coulomb barrier. This may indicate, as suggested also by the fusion cross section data, the occurrence of processes leading to large breakup cross sections of ${}^9\text{Be}$ since it has no bound states. Moreover the only inelastic channel observed was the well known collective multiplet $[{}^{208}\text{Pb}(3^-) \otimes h_{9/2}]_{J^\pi}$, visible only at 48 MeV and with small cross sections. All the other ${}^{209}\text{Bi}$ inelastic channels have negligible cross sections. The optical model potential, extracted from the elastic data fits, reproduces well also the inelastic excitations within a simplified CC approach.

We thank the staff of the Munich Tandem, especially W. Carli, for their professional operation of the accelerator and to H.J. Maier from the Technological Laboratory of the University of Munich and his staff for the target preparation. We also thank M.A. Nagarajan for discussion and comments on a first version of this manuscript.

-
- [1] I. Tanihata *et al.*, Phys. Lett. B **206**, 592 (1988); M. Fukuda *et al.*, *ibid.* **268**, 339 (1991).
- [2] A. Yoshida *et al.*, Phys. Lett. B **389**, 457 (1996).
- [3] Y. Y. Feng *et al.*, Nucl. Instrum. Methods Phys. Res. B **82**, 175 (1993).
- [4] C. Signorini *et al.*, Eur. Phys. J. A **2**, 227 (1998).
- [5] C. Signorini *et al.*, Eur. Phys. J. A **5**, 7 (1999).
- [6] M. DasGupta *et al.*, Phys. Rev. Lett. **82**, 1395 (1999).
- [7] M. V. Andrés, J. A. Christley, J. Gómez-Camacho, and M. A. Nagarajan, Nucl. Phys. **A612**, 82 (1997).
- [8] M. A. Nagarajan, J. Phys. G **23**, 1479 (1997).
- [9] N. Keeley, S. J. Bennett, N. M. Clarke, B. R. Fulton, G. Tungate, P. V. Drumm, M. A. Nagarajan, and J. S. Lilley, Nucl. Phys. **A571**, 326 (1994).
- [10] N. Keeley and K. Rusek, Phys. Lett. B **427**, 1 (1998).
- [11] V. Hnizdo, K. W. Kemper, and J. Szymakowski, Phys. Rev. Lett. **46**, 590 (1981).
- [12] V. Hnizdo, J. Szymakowski, K. W. Kemper, and J. D. Fox, Phys. Rev. C **24**, 1495 (1981).
- [13] M. A. Tiede, D. E. Trcka, and K. W. Kemper, Phys. Rev. C **44**, 1698 (1991).
- [14] A. Shrivastava, S. Kailas, P. Singh, A. Chatterjee, A. Narvin, A. M. Samant, V. Ramdev Raj, S. Mandal, S. K. Datta, and D. K. Awasthi, Nucl. Phys. **A635**, 411 (1988).
- [15] M. H. MacFarlane and S. C. Pieper, Argonne National Laboratory Report No. ANL-76-11, 1983, Rev. 1 (unpublished).
- [16] I. Thompson, Comput. Phys. Rep. **2**, 167 (1988).
- [17] R. Broglia and A. Winther, *Heavy Ion Reactions* (Benjamin, Reading, MA, 1984), p. 113.
- [18] D. P. Stahel *et al.*, Phys. Rev. C **16**, 1456 (1977).
- [19] M. A. Nagarajan, C. Mahaux, and G. R. Satchler, Phys. Rev. Lett. **54**, 1136 (1985).
- [20] C. Mahaux, C. Ngô, and G. R. Satchler, Nucl. Phys. **A449**, 354 (1986).
- [21] H. Gemmeke, B. Deluigi, L. Lassen, and D. Scholz, Z. Phys. A **A286**, 73 (1978).
- [22] D. Fick, G. Grawert, and I. M. Turkiewicz, Phys. Rep. **214**, 1 (1992).
- [23] M. J. Martin, Nucl. Data Sheets **63**, 723 (1991).